Modulated Raman spectroscopy for enhanced identification of bladder tumor cells in urine samples

Elisabetta Canetta
Michael Mazilu
Anna Chiara De Luca
Antonia E. Carruthers
Kishan Dholakia
Sam Neilson
Harry Sargeant
Tina Briscoe
C. Simon Herrington
Andrew C. Riches

Modulated Raman spectroscopy for enhanced identification of bladder tumor cells in urine samples

Elisabetta Canetta,[a] **Michael Mazilu,**[a] **Anna Chiara De Luca,**[a] **Antonia E. Carruthers,**[a] **Kishan Dholakia,**[a] **Sam Neilson,**[b] **Harry Sargeant,**[b] **Tina Briscoe,**[b] **C. Simon Herrington,**[b] **and Andrew C. Riches**[b]

[a]University of St Andrews, SUPA-School of Physics and Astronomy, North Haugh, St Andrews, KY16 9SS, United Kingdom
[b]University of St Andrews, School of Medicine, Medical and Biological Sciences Building, North Haugh, St Andrews, KY16 9TF, United Kingdom

Abstract. Standard Raman spectroscopy (SRS) is a noninvasive technique that is used in the biomedical field to discriminate between normal and cancer cells. However, the presence of a strong fluorescence background detracts from the use of SRS in real-time clinical applications. Recently, we have reported a novel modulated Raman spectroscopy (MRS) technique to extract the Raman spectra from the background. In this paper, we present the first application of MRS to the identification of human urothelial cells (SV-HUC-1) and bladder cancer cells (MGH) in urine samples. These results are compared to those obtained by SRS. Classification using the principal component analysis clearly shows that MRS allows discrimination between Raman spectra of SV-HUC-1 and MGH cells with high sensitivity (98%) and specificity (95%). MRS is also used to distinguish between SV-HUC-1 and MGH cells after exposure to urine for up to 6 h. We observe a marked change in the MRS of SV-HUC-1 and MGH cells with time in urine, indicating that the conditions of sample collection will be important for the application of this methodology to clinical urine samples. © *2011 Society of Photo-Optical Instrumentation Engineers (SPIE).* [DOI: 10.1117/1.3556722]

1 Introduction

Currently, a variety of diagnostic tests are used to detect bladder cancer.[1] However, these techniques are costly and time consuming for both hospitals and patients. In addition, most of these diagnostic tools require the expertise of a cytopathologist, radiologist (e.g., intravenous urography, computed tomography and magnetic resonance urography), or urologist (e.g., cystoscopy). This approach is the underlying reason for a "lack of progress" in the early diagnosis of bladder cancer.[1] A delay in the detection of invasive bladder cancer increases the risk of bladder cancer death.[2] Therefore, it is crucial to develop an inexpensive, noninvasive, highly sensitive, rapid, and easily automated technique to diagnose bladder cancer in its early stages.

In the last decade, Raman spectroscopy (RS) has been used for the discrimination of normal cells from bladder and prostate cancer cells on the basis of their biochemical fingerprints.[3] RS has considerable potential as a diagnostic tool for the classification of normal and cancer cells due to its noninvasive nature and capability to predict pathological diagnosis in real time.[4] However, the use of this spectroscopic technique is dramatically limited by the presence of strong fluorescence signals. These oc-

cur in the same spectral window as the inherently weak Raman signals from biomedical samples and therefore hide these Raman peaks. In the last 30 years several fluorescence-suppression methods have been developed, all with the aim of removing the fluorescence background and isolating the Raman signals.[5–11] These methods include polynomial fitting,[10] time-resolved Raman spectroscopy,[12] polarization modulation technique,[13] and shifted excitation Raman difference spectroscopy.[14] Though each of these techniques has been demonstrated to be useful in specific situations, they are not without limitations.

Recently, we developed a simple innovative method, modulated Raman spectroscopy (MRS), that is able to filter out the Raman spectra from the fluorescence background.[15, 16] The method is based on the wavelength shift of the Raman peaks as the wavelength of the excitation laser is continuously modulated while the fluorescence background remains static. By using an algorithm based on principal component analysis (PCA) of the raw data, mostly fluorescence-free Raman spectra are obtained. This method exposes even very weak Raman features generally masked by the fluorescence. Additionally, the signal-to-noise ratio of the modulated Raman spectra is greatly improved, reducing the necessary accumulation time and permitting real-time applications.

In this paper, we present the application of MRS to the identification of fixed urothelial and bladder tumor cells exposed to urine for up to 6 h. We model the effects of urine on exfoliated cells by using urothelial and malignant human bladder cell lines. We validate the use of the MRS technique to discriminate between fixed urothelial cells and cancer cells not exposed to urine

Address all correspondence to: Elisabetta Canetta, University of St Andrews, SUPA-School of Physics and Astronomy, St Andrews KY16 9SS, United Kingdom. Tel: +44 (0)1334 46 3124; Fax: +44 (0)1334 46 3104; E-mail: elisabetta.canetta@physics.org.

Michael Mazilu, University of St Andrews, SUPA-School of Physics and Astronomy, St Andrews, KY16 9SS, United Kingdom. Tel: +44 (0)1334 46 3210; Fax: +44 (0)1334 46 3104; E-mail: mm17@st-andrews.ac.uk.

Andrew C. Riches, University of St Andrews, School of Medicine, St Andrews, KY16 9TF, United Kingdom. Tel: +44 (0)1334 46 3603; Fax: +44 (0)1334 46 3482; E-mail: acr1@st-andrews.ac.uk.
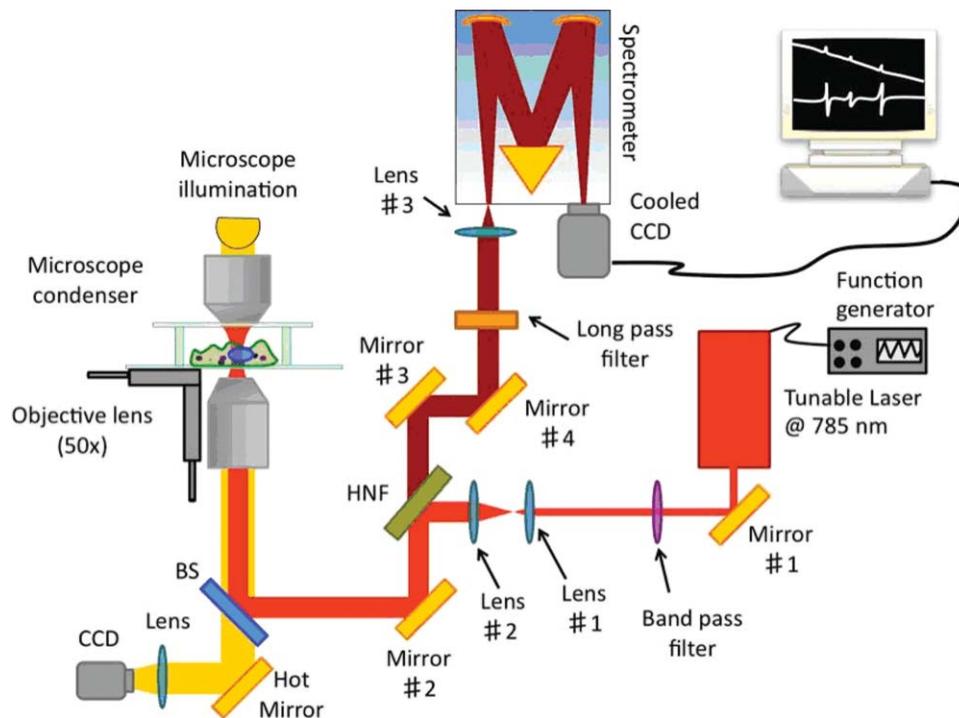
Fig. 1 Experimental setup (not to scale): A laser beam is expanded through a telescope formed by Lens #1 and Lens # 2 lenses and reflected from a 45° holographic notch filter (HNF) and focused on the sample by an objective lens (50×). The Raman scatter from the sample is collected by the same microscope objective and filtered by the same HNF. It is then guided toward the spectrometer and acquired *via* a liquid nitrogen cooled CCD camera.

by comparing modulated Raman (MR) spectra of these cells to the corresponding standard Raman (SR) spectra. The ability of MRS compared to standard Raman spectroscopy (SRS) to classify urothelial cells and cancer cells is then assessed by carrying out PCA on both the SR and MR spectra. We then mimic a scenario closer to a real clinical setting by exposing urothelial cells and bladder cancer cells to urine for different lengths of time up to 6 h. The ability of MRS to classify urothelial cells and cancer cells correctly in urine is assessed by multivariate analysis.

2 Materials and Methods

2.1 *Experimental Set-Up*

The MR microscopy system is shown in Fig. 1. The setup is identical to that used for standard Raman[17] but for the laser which is a tunable diode laser (Sacher Lasertechnik, TEC-520–0780-100, external cavity diode laser in a Littman configuration, total tuning range 25 nm) operating at 785 nm and with a maximum power of 100 mW. Additionally, an external arbitrary waveform/function generator (Keithley, 3390 50 MHz) is connected to the tunable laser to modulate the wavelength at frequencies as low as a few millihertz.

2.2 *Cell Lines and Sample Preparation*

Human urothelial cells (SV-HUC-1) were cultured in the following medium: F-12 nutrient mixture with L-glutamine (Ham-GIBCO 21765), with added human insulin 5 μg/ml, hydrocortisone 1 μg/ml, transferrin 5 μg/ml, glucose 2.7 mg/ml (Sigma), nonessential amino acids 0.1 mM (Gibco), penicillin 100 μg/ml, streptomycin 100 U/ml (Sigma), and fetal calf serum

1% (Globepharm). The SV-HUC-1 cells had been immortalized by transformation with simian virus 40 (SV40).[18]

A cell line derived from a recurrent human bladder tumor (MGH-U1) was maintained in long-term culture.[19] It has been shown that the MGH cell line is the same as the T24 cell line, also derived from a recurrent bladder tumor.[20] MGH-U1 cells were cultured in the following medium: GIBCO D-MEM:F12 (1:1) with added fetal calf serum 7% (Globepharm), penicillin 100 μg/ml, L-glutamine 2 mM, and streptomycin 100 U/ml (Sigma).

Cells from each cell line were incubated for up to 6 h in a fresh urine sample that had been filtered through a 0.22-μm Millipore filter. These samples were collected from healthy donors with full ethical approval (approval number MD5091). Cell viability was assessed by sampling the cells at different times in urine and incubating the cells with 1% Fast Green [CI (color index number) 42053, Sigma Chemical Co. Ltd.] for 5 min. The proportion of cells that excluded the dye was recorded.

Further samples incubated in urine were diluted in a large volume of medium and plated in microtiter plates to assess their reproductive capacity. Following 4 days culture, viability was assessed by adding 10 μl of cell counting reagent (Dojindo kit CK04) and incubating the plates for a further 3 h, after which the optical density was measured using a Dynex MRX reader at a wavelength of 450 nm.

To prepare the samples, cells from each cell line were incubated in urine for different lengths of time up to 6 h. At 0 h (control), 30 min, 3 and 6 h, PreservCyt (Cytec, UK) was added at a ratio of 2 parts urine to 1 part PreservCyt. The cells were then pelleted by centrifugation at 600 g for 10 min and resuspended in PreservCyt for storage at 4°C. Samples for Raman analysis were washed extensively in phosphate-buffered saline
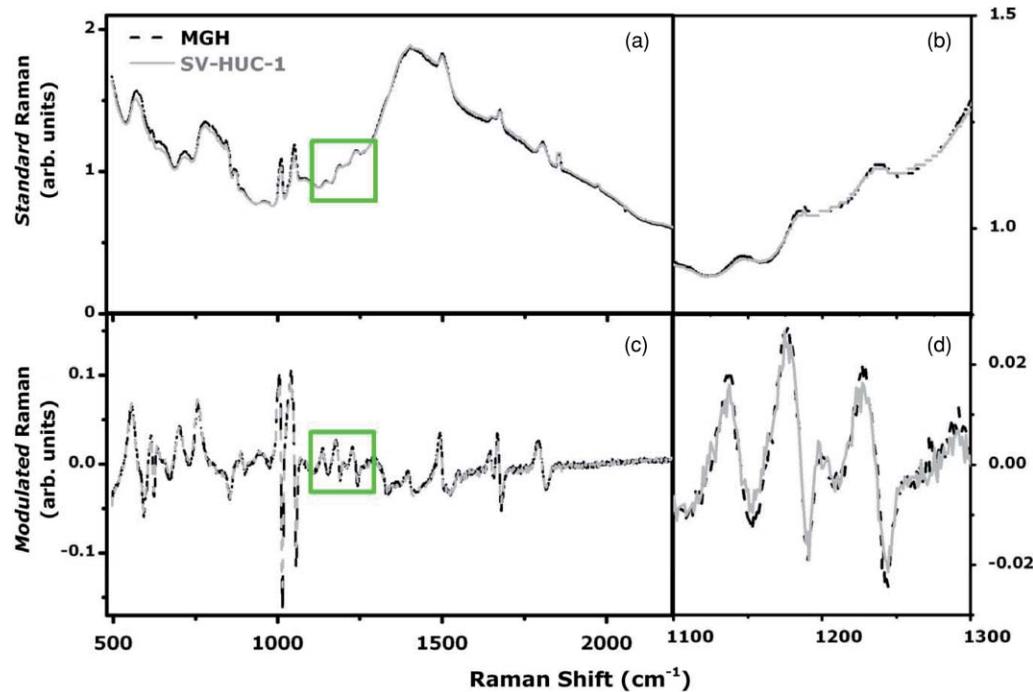
Fig. 2 (a) Mean standard Raman spectrum of fixed urothelial (SV-HUC-1) and bladder cancer cells (MGH) not exposed to urine (control). (b) Zoom on region 1100 to 1300 cm^{-1}. (c) Mean modulated Raman spectra of control fixed SV-HUC-1 and bladder cancer MGH cells. (d) Zoom on region 1100 to 1300 cm^{-1}.

(PBS) and re-suspended in 100 μl of PBS to concentrate the cells.

The sample chamber used in the Raman experiments was made by using a 80-μm deep vinyl spacer between a quartz slide (1 mm in thickness) and a quartz coverslip (150 μm in thickness) (UQG, United Kingdom). 20 μl of cell suspension was placed inside the chamber and the cells were allowed to sediment onto the inverted quartz coverslip for ~30 min before starting the Raman experiments.

2.3 *Method and Spectral Analysis*

Single cell standard spectra were acquired from 40 fixed urothelial cells (SV-HUC-1) and 40 fixed bladder cancer cells (MGH cells) exposed to urine for 0 h (control), 30 min, 3 and 6 h. The background spectra were also acquired. The laser power on the sample during signal acquisition was ~8 mW, and each spectrum was collected in the range from 500 to 2100 cm^{-1} with an integration time of 200 s. The laser beam, during acquisition, was focused on the cell nucleus.

For each cell, 40 stacked spectra were recorded with an acquisition time of 5 s each while the laser wavelength was modulated with a ramp wave of 50% symmetry, a modulation frequency of 40 mHz, and a modulation amplitude of 60 GHz (corresponding to 0.2 nm at this wavelength). The 40 stacked spectra were then analyzed by using a custom designed MATLAB script based on the PCA method for fluorescence suppression, and modulated Raman spectra of the cells were obtained. These modulation parameters were chosen to maximize the signal-to-noise ratio (data not shown). Indeed, higher modulation frequencies decrease the $1/f$ noise level while increasing the shot noise.[16]

To evaluate the SR and MR spectra of control and urine-stressed HUC and MGH cells and to compare different cell classes against each other, PCA[21] was carried out. The specificity/sensitivity and, more generally, the confusion matrix was determined using a leave-one-out procedure in which each spectrum is classified against the PCA of all the other spectra. The overall efficiency was defined as the proportion of cells classified correctly.

3 Results and Discussion

3.1 *Cell Viability*

The viability of both the urothelial cells and the bladder tumor cells decreased with time in urine as assessed by dye exclusion. After 1 h the viability decreased to $(60 \pm 2)\%$ for the tumor cells and $(64 \pm 4)\%$ for the urothelial cell line. In contrast, the reproductive capacity of both cells decreased rapidly after incubation in urine. After 20 min the tumor cells had almost completely lost reproductive integrity and the urothelial cells demonstrated a similar decline by 40 min.

3.2 *Standard and Modulated Raman Spectra for Control Fixed SV-HUC-1 and MGH Cells*

To test the robustness of the MRS technique compared to SRS, fixed urothelial cells (SV-HUC-1) and bladder cancer cells (MGH) not exposed to urine (control) were characterized by both MRS and SRS.

Figure 2 displays the mean Raman spectra obtained by SRS and MRS. SR spectra of SV-HUC-1 and MGH cells [Fig. 2(a)] show a strong fluorescence background generated from the quartz surfaces of the sample chamber and some cell autofluorescence. It is clear that SRS does not allow the finest details of the Raman features of the cells to be defined, thus making it difficult to assign precisely the various chemical constituents in
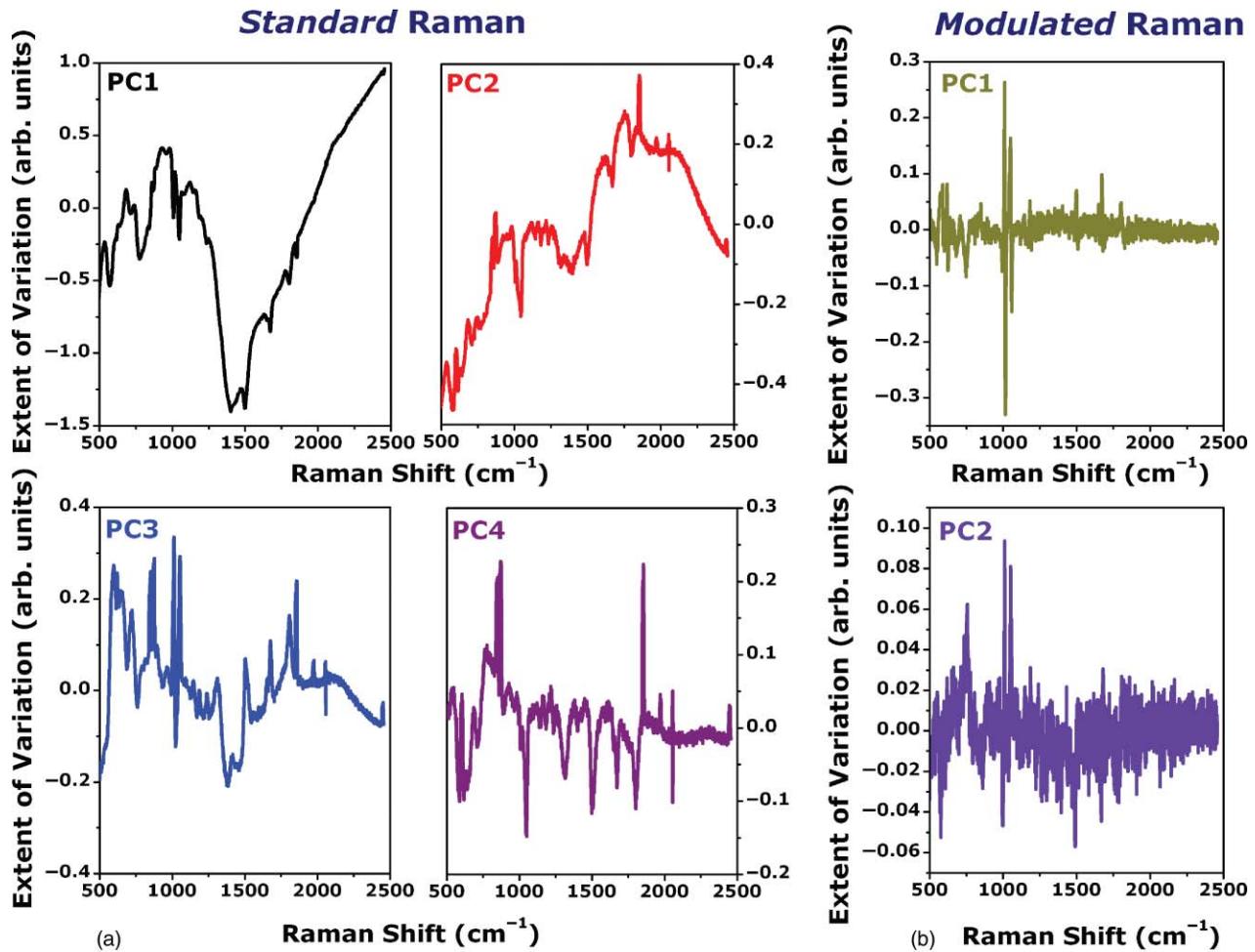
Fig. 3 (a) First four principal components generated by the analysis of SR spectra for control MGH cells. (b) First two principal components generated by the analysis of MR spectra for control MGH cells.

the analyzed sample [Fig. 2(b)]. Conversely, in the MR spectra of SV-HUC-1 and MGH cells [Fig. 2(c)] the Raman peaks of the chemical constituents of the cells can be clearly observed [Figs. 2(c) and 2(d)]. This facilitates the assignment of individual peaks based on previous data.[22] To carry out an objective comparison between the urothelial cell (SV-HUC-1) and cancer cell (MGH) spectra, each spectrum is normalized to the height of the double peak in the region 950 to 1100 cm^{-1}. This normalization is applied to the whole spectrum. Comparing the relative intensities of the spectral peaks for SV-HUC-1 and MGH spectra show that urothelial cells (SV-HUC-1) are characterized by relatively strong protein and carbohydrate Raman peaks, in the spectral region 1100 to 1300 cm^{-1}, which suggest greater concentrations of proteins and carbohydrates in nonmalignant cells.[23] In contrast, the spectra from bladder cancer cells (MGH) show a significant increase in the peaks pertaining to ring breathing modes in DNA bases, such as 669, 727, 785, 828, 1095, and 1578 cm^{-1}, suggesting an increase in the DNA concentration of bladder cancer cells. Tumor cells commonly exhibit an increase in DNA content in the nucleus.

The ability of modulated Raman spectroscopy, compared to standard Raman spectroscopy, to discriminate between control urothelial cells (SV-HUC-1) and bladder cancer cells (MGH) was assessed using PCA. In the PCA carried out on the SR and

MR spectra of the SV-HUC-1 and MGH cells, 40 SV-HUC-1 spectra were compared with 40 MGH spectra.

As clearly observed in Fig. 2(a), the standard spectra show a very strong background intensity (cell autofluorescence), upon which the Raman spectra are superimposed. This behavior is also clearly visible in the first two principal components shown in Fig. 3(a).

PC1 and PC2 of the SR spectra appear predominantly to describe the inter-sample variation in autofluorescence, which cannot be directly attributed to the cellular changes that distinguish the samples. To support this argument we used the Fourier transform (FT) to estimate the difference between the slow varying background and the sharp Raman bands. Indeed, the FT of a slowly varying signal contains only low frequency components while sharp/fast variations imply high frequency components. Here, we calculate the FT along the wavenumber axis of the first four principal component spectra. In the Fourier space the broad background signal is visible at low frequencies, while the sharp Raman peaks are present at high frequencies. Using this approach, we observe that the most important Raman variations between SV-HUC-1 and MGH standard spectra are given by the 3rd and 4th PCs and, therefore, the 1st and 2nd PCs are not taken into account. Thus, the discrimination between SV-HUC-1 and MGH standard spectra was based on the 3rd and 4th PCs as
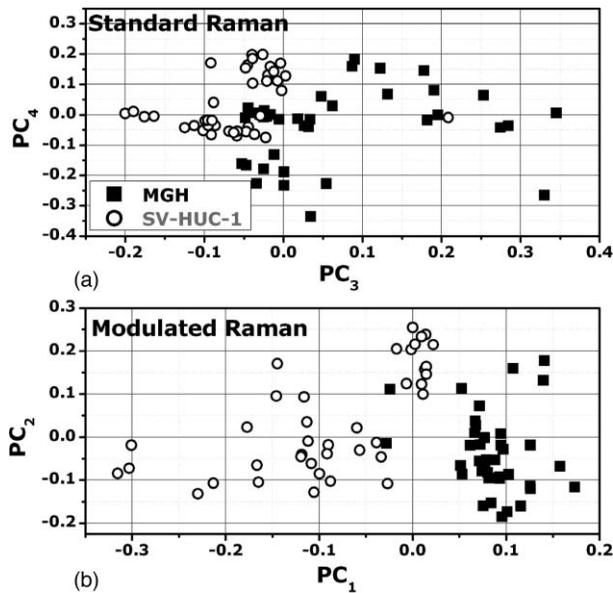
Fig. 4 (a) PCA of all individual SR spectra and (b) PCA of all individual MR spectra for 40 control SV-HUC-1 and 40 MGH cells.

shown in Fig. 4(a). The two cell types do not form distinct and separate clusters, giving a sensitivity of 97% and a specificity of 72%.

The spectra recorded via MR spectroscopy have advantages over the SR spectra when used in a multivariate analysis such as PCA. First, PCA relies on a normal distribution of the noise, which might not be the case for SR spectroscopy due to the positive nature of the spectral intensity. On the contrary, the MR spectra oscillate between negative and positive values [Fig. 2(b)] and therefore the noise of the MR spectra can have a normal distribution. Further, MR spectra are background-free and the Raman contribution is already present in the first two PCs as clearly observed in Fig. 3(b).

The plot of the first two main PCs for the MR spectra of SV-HUC-1 and MGH cells are shown in Fig. 4(b), revealing the presence of two very distinct clusters, one for SV-HUC-1 cells and the other for MGH cells. These findings indicate that when
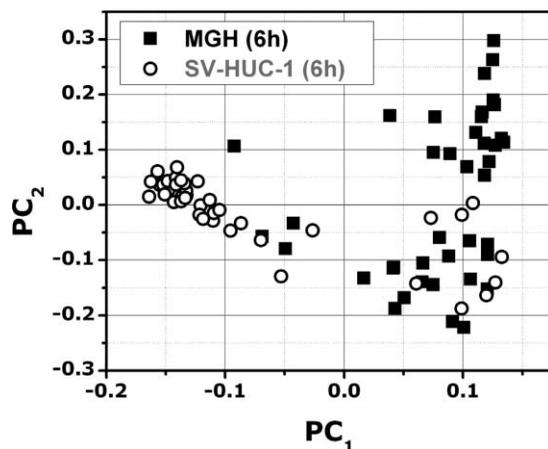
PCA is carried out on the MR spectra its ability to discriminate between SV-HUC-1 and MGH cells is improved. Therefore, the 1st and 2nd components, containing the most pertinent Raman information, can be used to discriminate between SV-HUC-1 and MGH modulated spectra resulting in excellent sensitivity (98%) and specificity (95%).

3.3 Modulated Raman Spectroscopy of Urine-Stressed Urothelial Cells (SV-HUC-1) and Bladder Cancer Cells (MGH)

To mimic a scenario as close as possible to a clinical setting, the effects of urine on the Raman spectra and hence the biochemistry of urothelial cells (SV-HUC-1) and bladder cancer cells (MGH) were investigated. The two types of cells were exposed to urine for different lengths of time up to 6 h and MR spectroscopy was carried out following fixation of the SV-HUC-1 and MGH cells.

First, 40 urine-stressed SV-HUC-1 cell spectra were compared with 40 urine-stressed MGH cell spectra to assess the ability of multivariate analyses of MR spectra to differentiate between SV-HUC-1 and MGH cells after exposing them to urine for 6 h. The plots of the first two PCs against each other for MR spectra of stressed SV-HUC-1 and MGH cells are shown in Fig. 5.

PCA comparing the MR spectra of HUC cells exposed to urine for 6 h show distinct, separate clusters for the two stressed cell types. Even after 6 h exposure sensitivity and specificity are quite high: 80% sensitivity and 87% specificity compared to the control (0 h in urine) samples (sensitivity: 98% and specificity: 95%). The reason for the decrease could be the detrimental effect of urine on the biochemistry of the cells causing a reduction of the signal-to-noise ratio in the MR spectra. Exposure to urine did affect the spectra, however multivariate analyses of the MR spectra could still discriminate between urothelial cells and bladder cancer cells which support the robustness of modulated Raman spectroscopy.

To gain a deeper understanding of the effect of urine on the biochemical signatures of SV-HUC-1 and MGH cells, 40
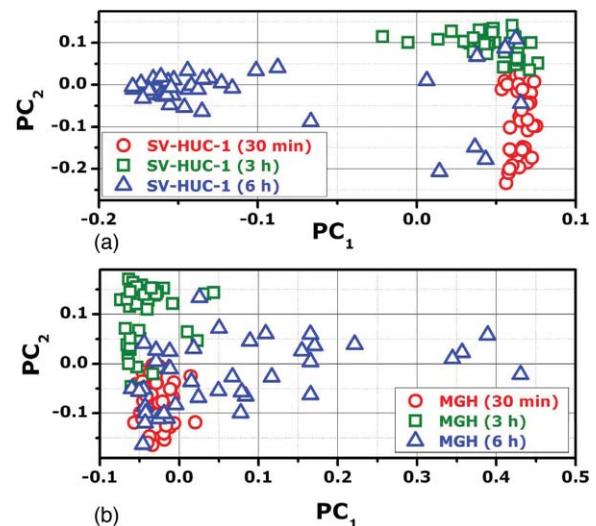

Fig. 5 PCA of all individual MR spectra for 40 SV-HUC-1 and 40 MGH cells exposed to urine for 6 h.

Fig. 6 PCA of individual MR spectra of (a) urine-stressed urothelial cells (SV-HUC-1) and (b) urine-stressed bladder cancer cells (MGH).

Table 1 Confusion matrix giving the classification for urine-stressed SV-HUC-1 and urine-stressed MGH.

	SV-HUC-1			MGH		
	Predicted classification					
True classification	30 min	3 h	6 h	30 min	3 h	6 h
30 min	39	1	0	29	2	9
3 h	2	36	2	2	34	4
6 h	4	3	33	4	3	33

urine-stressed SV-HUC-1 cell spectra from each time point were compared with each other to determine whether multivariate analyses can correctly predict how long the cells are exposed to urine [Fig. 6(a)]. The same analysis was carried out on 40 urine-stressed MGH cell spectra [Fig. 6(b)].

PCA comparing the MR spectra of normal SV-HUC-1 cells exposed to urine for 30 min, 3 and 6 h [Fig. 6(a)] shows distinct, separate clusters for each group of stressed cells. In particular, the cells exposed to urine for 6 h are distinctly separated from the other clusters, probably due to larger alterations of their biochemical signatures caused by the long exposure to urine. A similar trend can be observed for urine-stressed MGH cells [Fig. 6(b)] with well-separated clusters for each group of stressed cells. The separation of clusters of SV-HUC-1 cells is more pronounced than those from MGH cells, which may reflect differences in the rate of DNA breakdown and protein damage in the urine-stressed cells.

The main result of this analysis is the creation of a confusion matrix corresponding to the leave-one-out predictive classification of SV-HUC-1 after 30 min, 3 and 6 h exposure to urine (Table 1). The same confusion matrix was created for urine-stressed MGH cells (Table 1). By analyzing the diagonal values of the confusion matrixes for SV-HUC-1 and MGH, we can obtain an overall predictive efficiency of about 90% for the urine-stressed SV-HUC-1 and of about 75% for the stressed MGH. These results suggest that MGH bladder cancer cells are more sensitive to urine exposure than SV-HUC-1 urothelial cells. This is consistent with the rapid decrease in the cell viability and reproductive capacity of urine-stressed MGH cells compared to SV-HUC-1 cells.

4 Conclusions

MRS was applied to the discrimination of urothelial cells and bladder cancer cells from human cell lines exposed to urine.

The SR spectra of the control SV-HUC-1 and MGH cells were classified with an efficiency of 85%, while the corresponding MR spectra were identified with an efficiency of 97%, demonstrating the superiority of MRS over SRS for the characterization and classification of these cell types. We observed that MR spectra of urine-stressed urothelial cells and bladder cancer cells succeeded in correctly predicting how long the cells were exposed to urine with an efficiency of 95% for normal SV-HUC-1 cells and 97% for cancer MGH cells.

The high sensitivity, specificity, and efficiency obtained from multivariate analyses on MR spectra of urothelial cells and bladder cancer cells in urine demonstrates the great potential of MRS as a rapid, inexpensive, and accurate clinical tool to detect the presence of bladder cancer cells in urine samples.

References

1. M. Araki, A. M. Nieder, M. Manoharan, Y. Yang, and M. S. Soloway, "Lack of progress in early diagnosis of bladder cancer," *Urology* **69**(2), 270–274 (2007).
2. F. Liedberg, H. Anderson, Å. Månsson, and W. Månsson, "Diagnostic delay and prognosis in invasive bladder cancer," *Scand. J. Urol. Nephrol.* **37**(5), 396–400 (2003).
3. T. J. Harvey, C. Hughes, A. D. Ward, E. Correia Faria, A. Henderson, N. W. Clarke, M. D. Brown, R. D. Snook, and P. Gardner, "Classification of fixed urological cells using Raman tweezers," *J. Biophoton.* **2**(1–2), 47–69 (2009).
4. E. C. C. Cauberg, D. M. de Bruin, D. J. Faber, T. G. van Leeuwen, J. M. C. H. de la Rosette, and T. M. de Reijke, "A new generation of optical diagnostics for bladder cancer: technology, diagnostic accuracy, and future applications," *Eur. Urol.* **56**(2), 287–297 (2009).
5. A. Z. Genack, "Fluorescence suppression by phase-resolved modulation Raman-scattering," *Anal. Chem.* **56**(14), 2957–2960 (1984).
6. A. Shreve, N. Cherepy, and R. Mathies, "Effective rejection of fluorescence interference in Raman spectroscopy using a shifted excitation difference technique," *Appl. Spectrosc.* **46**(4), 707–711 (1992).
7. C. Xie and Y. Li, "Confocal micro-Raman spectroscopy of single biological cells using optical trapping and shifted excitation difference techniques," *J. Appl. Phys.* **93**(5), 2982–2986 (2003).
8. I. G. Cormack, M. Mazilu, K. Dholakia, and C. S. Herrington, "Fluorescence suppression within Raman spectroscopy using annular beam excitation," *Appl. Phys. Lett.* **91**(2), 023903 (2007).
9. J. Zhao, H. Lui, D. McLean, and H. Zeng, "Automated fluorescence background subtraction algorithm for biomedical Raman spectroscopy," *Appl. Spectroscop.* **61**(11), 1225–1232 (2007).
10. B. Beier and A. Berger, "Method for automated background subtraction from Raman spectra containing known contaminants," *Analyst.* **134**(6), 1198–1202 (2009).
11. G. Rusciano, A. C. De Luca, G. Pesce, and A. Sasso, "Phase-sensitive detection in Raman tweezers," *Appl. Phys. Lett.* **89**(26), 261116 (2006).
12. F. Knorr, Z. J. Smith, and S. Wachsmann-Hogiu, "Development of a time-gated system for Raman spectroscopy of biological samples," *Opt. Express* **18**, 20049–20058 (2010).
13. S. M. Angel, M. K. Dearmond, K. W. Hanck, and D. W. Wertz, "Computer-controlled instrument for the recovery of a resonance Raman spectrum in the presence of strong luminescence," *Anal. Chem.* **56**, 3000–3001 (1984).
14. S. T. McCain, R. M. Willett, and D. J. Brady, "Multi-excitation Raman spectroscopy technique for fluorescence rejection," *Opt. Express* **16**, 10975–10991 (2008).
15. A. C. De Luca, M. Mazilu, A. C. Riches, C. S. Herrington, and K. Dholakia, "Online fluorescence suppression in modulated Raman spectroscopy," *Anal. Chem.* **82**(2), 738–745 (2010).
16. M. Mazilu, A. C. De Luca, A. C. Riches, C. S. Herrington, and K. Dholakia, "Optimal algorithm for fluorescence suppression of modulated Raman spectroscopy," *Opt. Express* **18**(11), 11382–11394 (2010).
17. P. R. T. Jess, M. Mazilu, K. Dholakia, A. C. Riches, and C. S. Herrington, "Optical detection and grading of lung neoplasia by Raman microspectroscopy," *Int. J. Cancer* **124**(2), 376–380 (2009).

18. B. J. Christian, L. J. Loretz, T. D. Oberley, and C. A. Reznikoff, "Characterisation of human uroepithelial cells immortalised in vitro by simian virus 40," *Cancer Res* **47**(22), 6066–6073 (1987).

19. J. R. W. Masters and P. J Hepburn, "Human bladder cancer in vitro drug sensitivities: Range and stability in long-term culture," *Br. J. Cancer* **54**, 131–135 (1986).

20. C. M. O'Toole, S. Povey, P. Hepburn, and L. M. Franks, "Identity of some human bladder cancer cell lines," *Nature (London)* **301**(5899), 429–430 (1983).

21. J. W. Chan, D. S. Taylor, T. Zwedling, S. M. Lane, K. Ihara, and T. Huser, "Micro-Raman spectroscopy detects individual neoplastic and normal hematopoietic cells," *Biophys. J.* **90**(2), 648–656 (2006).

22. I. Notingher, "Raman spectroscopy cell-based biosensors," *Sensors* **7**(8), 1343–1358 (2007).

23. P. R. T. Jess, D. D. W. Smith, M. Mazilu, K. Dholakia, A. C. Riches, and C. S. Herrington, "Early detection of cervical neoplasia by Raman spectroscopy," *Int. J. Cancer* **121**(12), 2723–2728 (2007).